8-28-2000

# AlGaN/GaN Metal-Oxide-Semiconductor Heterostructure Field-Effect Transistors on SiC Substrates

M. Asif Khan

X. Hu

A. Tarakji

Grigory Simin
*University of South Carolina - Columbia*, simin@engr.sc.edu

J. Yang

*See next page for additional authors*

**Author(s)**
M. Asif Khan, X. Hu, A. Tarakji, Grigory Simin, J. Yang, R. Gaska, and M. S. Shur

# AlGaN/GaN metal–oxide–semiconductor heterostructure field-effect transistors on SiC substrates

M. Asif Khan, X. Hu, A. Tarakji, G. Simin, J. Yang, R. Gaska, and M. S. Shur

## Articles you may be interested in

AlGaN/GaN polarization-doped field-effect transistor for microwave power applications
Appl. Phys. Lett. **84**, 1591 (2004); 10.1063/1.1652254

Delta-doped AlGaN/GaN metal–oxide–semiconductor heterostructure field-effect transistors with high breakdown voltages
Appl. Phys. Lett. **81**, 4649 (2002); 10.1063/1.1527984

Comparative study of drain-current collapse in AlGaN/GaN high-electron-mobility transistors on sapphire and semi-insulating SiC
Appl. Phys. Lett. **81**, 3073 (2002); 10.1063/1.1512820

Gate leakage effects and breakdown voltage in metalorganic vapor phase epitaxy AlGaN/GaN heterostructure field-effect transistors
Appl. Phys. Lett. **80**, 3207 (2002); 10.1063/1.1473701

Mechanism of radio-frequency current collapse in GaN–AlGaN field-effect transistors
Appl. Phys. Lett. **78**, 2169 (2001); 10.1063/1.1363694

# AlGaN/GaN metal–oxide–semiconductor heterostructure field-effect transistors on SiC substrates

M. Asif Khan,[a] X. Hu, A. Tarakji, G. Simin, and J. Yang
*Department of Electrical and Computer Engineering, University of South Carolina, Columbia, South Carolina 29208*

R. Gaska
*Sensor Electronic Technology, Inc., Latham, New York 12110*

M. S. Shur
*CIEEM and Department of ECSE, Rensselaer Polytechnic Institute, Troy, New York 12180*

We report on AlGaN/GaN metal–oxide–semiconductor heterostructure field-effect transistors (MOS-HFETs) grown over insulating 4H–SiC substrates. We demonstrate that the dc and microwave performance of the MOS-HFETs is superior to that of conventional AlGaN/GaN HFETs, which points to the high quality of $SiO_2$/AlGaN heterointerface. The MOS-HFETs could operate at positive gate biases as high as $+10$ V that doubles the channel current as compared to conventional AlGaN/GaN HFETs of a similar design. The gate leakage current was more than six orders of magnitude smaller than that for the conventional AlGaN/GaN HFETs. The MOS-HFETs exhibited stable operation at elevated temperatures up to $300\,°C$ with excellent pinch-off characteristics. These results clearly establish the potential of using AlGaN/GaN MOS-HFET approach for high power microwave and switching devices. © *2000 American Institute of Physics.* [S0003-6951(00)04635-0]

The development of new generations of GaN/AlGaN high temperature microwave power electronics requires field-effect transistors (FETs) with low gate leakage and superior pinch-off characteristics, specifically at elevated temperatures.[1] These properties directly impact the device drain breakdown voltage, rf performance, and noise figure. In the past, several groups have attempted to achieve gate leakage suppression and superior pinch-off characteristics using the metal–insulator–semiconductor FET (MISFETs)[2–4] or metal–oxide–semiconductor FETs (MOSFETs)[5] device approach. However, the performance level of all these insulated gate devices was well below that of the state-of-the-art AlGaN/GaN HFETs. More recently, we demonstrated AlGaN/GaN metal–oxide–semiconductor heterostructure field-effect transistors (MOSHFETs) on sapphire and reported on their dc characterization results.[6] Our MOSHFET design combines the advantages of the MOS structure which suppresses the gate leakage current and AlGaN/GaN heterointerface, which provides high-density high-mobility two-dimensional (2D) electron gas channel. The MOSHFET approach also allows for application of high positive gate voltages to further increase the sheet electron density in the 2D channel and hence the device peak currents.

These features make MOSHFETs extremely promising for high-power microwave applications. However, these applications place severe constrains on device thermal management, which can only be addressed with high thermal conductivity SiC substrates. In this letter, we now report on fabrication and characterization of AlGaN/GaN MOSHFETs over insulating 4H–SiC substrates. Saturation current as high as 1.3 A/mm with a gate leakage current as low as 100 pA at $-20$ V gate bias for $2\times150\,\mu m$ devices is measured. The microwave and high temperature performance of the MOSHFETs is also reported.

The built-in channel of our MOSHFET is formed by the high density 2D electron gas at the AlGaN/GaN interface as in regular AlGaN/GaN HFETs. However, in contrast to HFETs the metallic gate is isolated from AlGaN barrier layer by a thin $SiO_2$ film. Thus the MOSHFET gate behaves more like a MOS structure rather than a Schottky barrier used in regular HFETs. Since the properly designed AlGaN barrier layer is fully depleted by electron transfer to the adjacent GaN layer, the gate insulator in MOSHFET consists of two sequential layers: $SiO_2$ film and AlGaN epilayer. This double layer insulator provides extremely low gate leakage current and allows for a large negative to positive gate voltage swing. Due to the wide band gap and to the full depletion of the AlGaN barrier neither electron nor hole parasitic channel forms at $SiO_2$–AlGaN interface at the gate voltages up to $+10$ V. The absence of the parasitic channel is confirmed by our simulations and by the measured capacitance–voltage ($C$–$V$) and current–voltage ($I$–$V$) characteristics discussed below.

The device epilayer structure (see inset of Fig. 1) was grown by low-pressure metal-organic chemical vapor deposition (MOCVD) on insulating 4H–SiC substrate. All AlGaN/GaN layers for this structure were deposited at $1000\,°C$ and 76 Torr. A 50 nm AlN buffer layer was first grown at a temperature of $1000\,°C$, followed by a 0.4 $\mu m$ insulating GaN layer and a 50 nm $n$-GaN layer with an estimated doping level of $(2-5)\times10^{17}\,cm^{-3}$. The heterostruc-
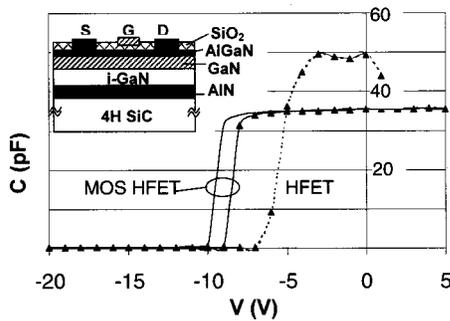
[a] Electronic mail: asif@engr.sc.edu

FIG. 1. $C-V$ plots for equal area 100 $\mu$m$\times$200 $\mu$m contacts on MOSHFET (solid curve) and HFET (dashed curve) structures. Solid and dashed lines represent $C-V$ dependence for MOSHFET and HFET structures correspondingly under illumination. Lines marked with triangles show the $C-V$ dependencies in the dark. The inset shows a schematic structure of AlGaN/GaN MOSHFET on 4H–SiC.
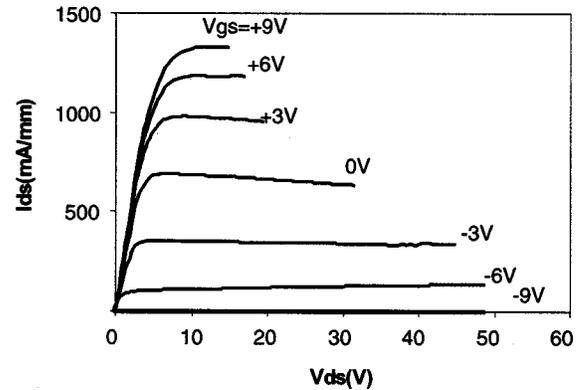


FIG. 2. $I-V$ characteristics for MOSHFET at room temperature. The gate length is 2 $\mu$m; the drain to source opening is 5 $\mu$m.

ture was capped with a 30 nm $Al_{0.2}Ga_{0.8}N$ barrier layer, which was doped with silicon approximately to $2\times10^{18}$ cm$^{-3}$. We also had a low-level flux of trimethylindium (TMI) present during the growth of all the layers of the structure. The presence of the indium surfactant, we believe, helps in improving the surface and interface roughness by incorporation of trace amounts of indium. The measured room temperature Hall mobility and sheet carrier concentration were 1150 cm$^2$/V s and $1.2\times10^{13}$ cm$^{-2}$.

Transistor devices were then fabricated using Ti(200A)/Al(500A)/Ti(200A)/Au(1500A) for the source-drain ohmic contacts. These were annealed at 850 °C for 1 min in nitrogen ambient. A multiple He implant with energies of 10, 50, and 100 keV and a dose of $(1-2)\times10^{15}$ cm$^{-2}$ was then used for device isolation. Prior to the gate fabrication, a 10 nm SiO$_2$ layer was deposited on part of the heterostructure using plasma enhanced chemical vapor deposition. The thickness of this layer, $d_{OX}$, was extracted from the $C-V$ measurement at 1 MHz on areas with and without the SiO$_2$ layer. In Fig. 1 we include the $C-V$ plots for 100 $\mu$m$\times$200 $\mu$m pads over the HFET and MOSHFET regions. From the zero volt capacitance of these metal–semiconductor structures (without SiO$_2$ layer), and using AlGaN layer permittivity $\epsilon_B$ = 8.8, we estimate the AlGaN barrier thickness $d_B$ to be 31 nm. This is very close to the 30 nm value estimated from the deposition rate. We then estimated the oxide thickness $d_{OX}$ from the following equation:

$$C_{MOS}=C_{MS}^*\left(\frac{1}{1+\dfrac{d_{OX}}{d_B}\cdot\dfrac{\epsilon_B}{\epsilon_{OX}}}\right). \qquad (1)$$

Here $C_{MOS}$ and $C_{MS}$ are the capacitances of equal area pads on the oxide and nonoxide areas and $\epsilon_{OX}=3.9$ is the SiO$_2$ dielectric permittivity. Using the data of Fig. 1 and Eq. (1) the SiO$_2$ thickness, $d_{OX}$, was estimated to be 7 nm. This is in reasonable agreement with the $d_{OX}$ value of 10 nm expected from deposition rate. In Fig. 1, we also include the $C-V$ characteristics measured under a strong white light illumination. As seen, for the HFET structure (without the SiO$_2$ layer), the $C-V$ curves in light and dark practically coincide. However, for the MOSHFET structure a threshold voltage shift $\Delta V\sim1$ V is measured. We attribute this voltage shift to the charge $\Delta Q=C\Delta V$ induced near the SiO$_2$/AlGaN inter-

face. Using the MOSHFET device capacitance measured at $V\approx-9$ V (see Fig. 1), we estimate the upper limit on surface charge density in SiO$_2$ layer, $n_s\approx10^{12}$ cm$^{-2}$. This is more then an order of magnitude less than the sheet carrier density (of free carriers) in the 2D channel of the MOSHFET, thereby indicating a high quality for the SiO$_2$/AlGaN interface.

We then fabricated Pt(200A)/Au(1000A) gate on both the regions with and without SiO$_2$. Gate length and widths were 2 and 100 $\mu$m, respectively. Figure 2 shows the measured $I-V$ characteristics of a device with oxide layer under the gate of AlGaN/GaN MOSHFET. The data of Fig. 2 are for the devices with a source-drain separation of 5 $\mu$m and the gate length of 2 $\mu$m. As seen, the maximum device current close to 1.3 A/mm was measured at a positive gate bias of +9 V. Further, the devices completely pinched off around $-9$ V. Assuming the maximum sheet carrier density in the undoped two-dimensional electron gas (2DEG) channel, limited by the 2D density of states, $n_s$, is about $2\times10^{13}$ cm$^{-2}$[7] and the electron drift velocity in the channel, $v=5\times10^6$ cm/s, we estimate the maximum achievable channel current $I_{sm}/W=q\times n_s\times v\approx1.6$ A/mm. Therefore the measured saturation current in our MOSHFET is close to this maximum value.

Figures 3(a) and 3(b) compare the transfer characteristics of AlGaN/GaN MOSHFET and baseline AlGaN/GaN HFET devices fabricated on the same wafer. At the positive gate bias of +2 V, the saturated current of approximately 0.9 A/mm was measured both for the HFET and MOSHFET
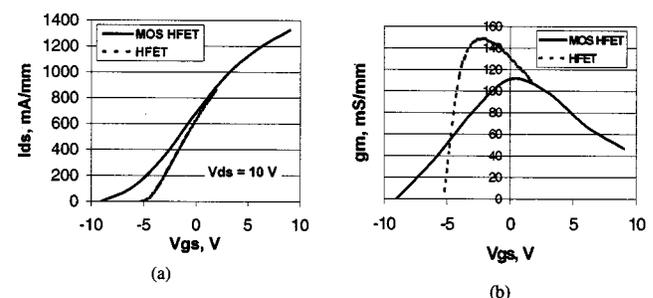


FIG. 3. The saturation-current (a) and transconductance (b) in the saturation region for the MOSHFET and baseline HFET devices. Drain to source voltage is 10 V. Device dimensions are the same as in Fig. 2.
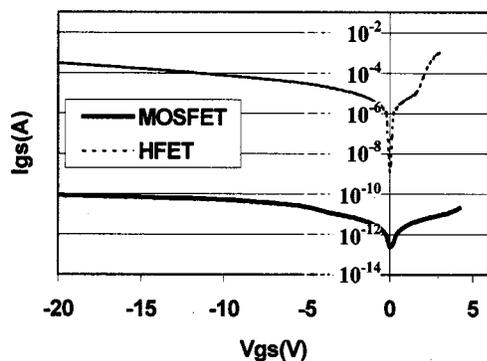
FIG. 4. Gate leakage current for the MOSHFET and the baseline HFET.

devices. As expected from the larger total barrier thickness and the lower dielectric constant of the $SiO_2$ layer, the MOSHFET transconductance is smaller than that of the baseline HFET device [see Fig. 3(b)]. The maximum transconductance, $g_m$ of 110 and 145 mS/mm, was measured for the 2 $\mu$m gate MOSHFET and baseline HFET devices, respectively. As seen from Fig. 3, the increased gate-to-channel separation is also responsible for the more negative threshold voltage of the MOSHFET. The MOSHFET also has an advantage of a much larger (nearly doubled) gate voltage swing and a higher linearity than the baseline HFET. This should, in principle, lead to a smaller intermodulation distortion, a smaller phase noise, and a larger dynamic range.

In Fig. 4, we show the gate leakage current for the two device types with an identical geometry (2 $\mu$m×200 $\mu$m gate area). The data shows that at room temperature the MOSHFET leakage current is as low as 100 pA at −20 V gate bias and is approximately six orders of magnitude smaller than for the HFET with similar gate dimensions. The pinch-off characteristics of AlGaN/GaN MOSHFET were measured in the temperature range 25–300 °C. The pinch-off current as low as 0.15 nA/mm at room temperature and 38 $\mu$A/mm at 250 °C was measured at the gate voltage $V_g = -15$ V and the drain bias of 10 V. Even at temperatures as high as 300 °C the pinch-off current remains approximately 10 mA/mm, which is about two orders of magnitude less than the maximum saturation current. No degradation was observed in the maximum saturation current up to 300 °C. The results of Figs. 3 and 4 clearly establish the potential of using our MOSHFET devices for high voltage, high temperature applications.

We also measured the current gain as a function of frequency using HP-8510 S-parameter analyzer. The cutoff frequency ($f_t$) values of 8.2 and 5.9 GHz were measured for the 2 $\mu$m gate MOSHFET and the HFET, respectively. Note that the value of the ($f_t \cdot L_g$) product of 16.4 GHz $\mu$m for MOSHFET also compares very favorably with the highest reported values for the state-of-the-art AlGaN/GaN HFETs.[8]

We also compared the maximum output rf power for both MOSHFET and HFET devices. The load-pull measurements were performed at 2 GHz using a Maury Microwave automated tuner system. Under identical bias conditions, 30 V drain bias and −1.5 V gate bias, the maximum power of about 2 W/mm was measured for both device types. Our data thus clearly indicates that the MOSHFET device approach preserves the high frequency and high power performance. We believe that the rf power characteristics of MOSHFETs might far exceed those of HFETs. The gate bias for MOSHFETs can be optimized to allow much higher input voltage and channel current swings. This should in principle lead to a much higher output power sweep compared to a similar geometry HFET without any significant transconductance collapse (see Fig. 2). Also, due to the low gate leakage current, the maximum drain voltage for MOSHFET can be higher than that for HFET, which may further increase the maximum rf power. A more detailed study of MOSHFET rf characteristics for a large periphery and submicron gate devices is currently underway and will be published elsewhere.

In conclusion, we demonstrated high performance $SiO_2$/AlGaN/GaN/SiC MOSHFETs with stable operation at elevated temperatures up to 300 °C. The measured dc, rf, rf power, and high temperature characteristics of the MOSHFET are equal to or better than for identical geometry HFET devices. This clearly establishes the feasibility of the AlGaN/GaN MOSHFET device approach for high-frequency, high-temperature, high-speed switching applications.

[1] N. Maeda, T. Saitoh, K. Tsubaki, T. Nishida, and N. Kobayashi, Jpn. J. Appl. Phys., Part 2 **38**, L987 (1999).
[2] M. Asif Khan, J. N. Kuznia, A. R. Bhattarai, and D. P. Olson, Mater. Res. Soc. Symp. Proc. **281**, 769 (1993).
[3] M. Asif Khan, M. S. Shur, Q. C. Chen, and J. N. Kuznia, Electron. Lett. **30**, 2175 (1994).
[4] S. C. Binari, L. B. Rowland, G. Kelner, W. Kruppa, H. B. Dietrich, K. Doverspike, and D. K. Gaskill, ''DC, Microwave, and High-Temperature Characteristics of GaN FET Structures,'' in *International Symposium Compound Semiconductors*, edited by H. Goronkin (IOP, Bristol, 1995), p. 459.
[5] F. Ren, M. Hong, S. N. G. Chu, and M. A. Marcus, M. J. Schurman, A. Baca, S. J. Pearton, and C. R. Abernathy, Appl. Phys. Lett. **73**, 3893 (1998).
[6] M. Asif Khan, X. Hu, G. Simin, A. Lunev, J. Yang, R. Gaska, and M. S. Shur, IEEE Electron Device Lett. **21**, 63 (2000).
[7] M. S. Shur, A. D. Bykhovski, and R. Gaska, Solid-State Electron. **44**, 205 (2000).
[8] R. Li, S. J. Cai, L. Wang, Y. Chen, K. L. Wang, R. P. Smith, S. C. Martin, K. S. Boutros, and J. M. Redwing, IEEE Electron Device Lett. **30**, 323 (1999).